Assessing the Solar Activity and Geomagnetic Disturbance during Minimum Phase of Solar Cycle 24 across the Globe.

Ajose Anthony Segara[1], Kayode Yusuf Olanrewaju[1], Alomaja Adegoke Jude[2]

[1]Department of Physics, Lagos State University of Education, Ijanikin, Lagos.

[2]Department of Physics, Lagos State University, Ojo, Nigeria.

DOI: https://doi.org/10.51584/IJRIAS.2023.81219

Received: 04 December 2023; Accepted: 12 December 2023; Published: 15 January 2024

ABSTRACT

Understanding solar activity and its implications on the Earth's environment has become necessary. Most importantly, events that characterized the minimum phase of solar cycle 24 (2019) and geomagnetic disturbance experienced during this period calls for an assessment. To assess this, the study has therefore used INTERMAGNET data from geomagnetic stations across the globe during the solar minimum year of solar cycle 24. A total of nine geomagnetic stations data of five disturbed days in a month were used, and were averaged in a minute interval for year 2019. The stations were selected with reference to their geomagnetic locations (latitudes and longitudes) as well as analyzing their horizontal magnetic field (H-Component) from the X and Y component of the geomagnetic field to reveal the variance in the global pattern of solar variations. The seasonal variations were studied across various latitudes and longitudes to understand the impact of solar activities on the earth surface as a result of geomagnetic field disturbance on Earth's magnetosphere at the end of cycle 24 (2019). The results of stations revealed ABK and DRV with 350nT and 150nT of H component respectively which are the highest while other stations have 60nT below. This study shows that low geomagnetic disturbance was witnessed during the end of the cycle due to the minimum solar activity which was as a result of low number of sunspot during this period.

Keywords: solar cycle, solar activity, sunspot, ionosphere, geomagnetic storm

INTRODUCTION

Solar activity has been associated with the number of sunspots on the Sun which occurs and runs over an 11-year interval called solar cycle (Hathaway, 2015; Petrovay, 2020; Efimenko and Lozitsky, 2023). Since sunspots are what determine the activities of the Sun which include flares, aurora, and other rapid releases of energy that can heat localized regions of the atmosphere (Gopalswamy, 2022; Miroshnichenko,2023). These activities of the Sun which is many millions of Kelvin, depicts the solar cycle and also describes the level of activity and variability of the Sun (Moldwin 2008). Since the amount of solar activity follows this sunspot or solar cycle, it is expected that the number of solar disturbances that impact Earth would also follow this cycle. Therefore, there will be variations in the space weather which is seasonal, with solar maximum indicating a strong likelihood of severe space weather and solar minimum predominantly quiet space weather. As a result of this variations, the seasonal changes on Earth's environment occurs because the earth resides in the outer atmosphere of the Sun and so our space environment is intimately connected to the structure and dynamics of the Sun (Gray et al., 2010; Moldwin,2022).

The sunspot through which coronal mass ejection (CME) is been ejected to generate geomagnetic induced currents (GICs) on the operation of technological systems such as power grids, communication cables, oil pipelines, and human health) depends on the number of spots (Pulkkinen et al., 2010). Coronal mass ejections are heavy expulsions of charged plasma which are been released from the solar atmosphere. These CMEs moving into interplanetary space influence geo-effectiveness of the Earth. They arrive at the Earth and interact with the Earth's magnetosphere resulting in geomagnetic storms, having influence from the magnetosphere to the ground (Falayi et al., 2017).

The beginning of the solar cycle marks the period when the sunspot starts to develop while the middle of every solar cycle marks the period when the sunspot has grown to the highest number on the sun's surface (Campbel, 2003). At the commencement of the solar cycle, there is a minimum number of sunspots, therefore the ejection rate is minimal which means solar activity on space weather will be predominantly lower (Howard, 2014; Ishkov,2018, 2021). In other cases, in the middle of the solar cycle when the sunspot is at its peak, ejection is high giving rise to maximum solar activity resulting in a high induction rate which could affect technological systems. The end of the solar cycle behaves the same way as the beginning of the cycle, therefore strong geomagnetic storms are not expected at this period (Reyes et al., 2021; Owens et al., 2021)

However, during a geomagnetic storm, electric currents flowing within both the magnetosphere and ionosphere influence the earth's geomagnetic field, causing variations in its components (H ,D, Z) which extends to low magnetic latitudes (Yamazaki, et al., 2011). This influence is observed as a disturbance on the magnetic component measured at intervals as a Disturbance Storm Time (dst), taken to be one of the major parameters used to measure the strength of a geomagnetic storm. The horizontal geomagnetic component H can be used to obtain the disturbance storm time at different latitudes (Ajose and Falayi, 2019). Falayi and Bolaji, (2016) also emphasized the major driver for geomagnetically induced current is the horizontal electric field induced at the Earth's surface as a result of time-dependent ionospheric current systems.

Solar activity affects terrestrial climate, though the changes in the total solar irradiance may seem not to produce much significant effect on the Earth's atmosphere (Yamazaki and Kosch, 2014). However, Haigh, (2007) opined that the Earth's climate heat and cool is as a result of solar activity rise and fall. If this happens, this study assesses the end of solar cycle 24 (2019) at which the number of sunspots will be at minima, but to what level will the solar activity reveal during this period has been a major challenge in recent time. This study will therefore probe the variations caused by the horizontal component H(dH) to ascertain the induction rate and geomagnetic disturbance on the earth's magnetic field. This gives room to explain solar activity as an experience of the Earth's environment.

Although study have shown that solar cycle 24 which commenced in December 2008 and ended in May 2020 was marred with low minimum activity (Watari 2017). The maximum sunspot number was 116.4 according to the World Data Center for Sunspot Index and this happened to be the smallest value ever observed since the maximum of solar cycle 14 (SSN of 107.1 in February 1906). Solar cycle 24 shows two peaks (solar maximum) with sunspot number 98.3 in March 2012 and 116.4 in April 2014 (Watari 2017). The two-peak variation of geomagnetic activities seen in the previous cycles according to Echer et al., (2011) stated that the first peak is caused by Coronal Mass Ejections (CMEs) and the second peak is caused by High-Speed Streams (HSSs) from coronal holes. Watari (2017) was able to confirm the same factor responsible for two solar maximums in cycle 24.

This study therefore examines the solar activity that ends cycle 24 and is expected to reveal the impact on the Earth's environment.

MATERIALS AND METHODS OF ANALYSIS

The data set for this study was INTERMAGNET from nine geomagnetic stations during the year 2019. This year marks the end of solar cycle 24 to observe the kind of activity that ended the cycle. Nine stations were selected with different geomagnetic locations as shown in table 1, across the globe to explain the solar activity as experienced at different locations around the world.

Table 1. Study stations with their locations

Stations Name	Station Code	Geomagnetic Latitude	Geomagnetic Longitude	Country Location
Alma Ata	AAA	43.2	76.9	Kazakhstan
Abisko	ABK	21.64	18.82	Sweden
Ascension	ASC	-8.0	345.6	Britain
Boulder	BOU	40.137	254.76	USA
Dumontd' Urville	DRV	-66.65	140.01	France
Eskladimur	ESK	55.314	356.79	UK
Hermanus	HER	-34.4	19.2	South Africa
Kourou	KOU	5.21	307.27	France
Uppsala	UPS	59.9	17.4	Sweden

Five disturb days were selected for each station during the year. The H component in Nano Tesla (nT) is computed from X and Y component of geomagnetic field and is used for the computations of the five disturbed days from equation 1.

$$H = \sqrt{X^2 + Y^2} \qquad (1)$$

The averages of the minute records of the geomagnetic elements of the H were taken for these five days and were obtained to represent the disturbed days for one month (Campbel 2003). This represents the characteristic behavior observed for each month of the year for all the stations.

The baseline value is used to determine the mean of the horizontal component H for a day (01.00LT– 24.00 LT) of the geomagnetic field. This is carried out using equation 2

$$H_{BL} = \frac{H_{01} + H_{02} + H_{023} + H_{024}}{4} \qquad (2)$$

where H_{BL} is the baseline value. The hourly variation *(dH_h)* at 24.00LT on H is then determined using equation 3.

$$dH_h = H_h - H_{BL} \qquad (3)$$

where H_h is the hourly correction of the minute data (Rabiu, et al., 2007, Obiekezie, et al., 2013). The dH is therefore obtained for all the stations across the year 2019. These values show the variation which is represented in the plots in the next section.

RESULT AND DISCUSSION

The Analysis of Variance of the H Component

The results obtained from the analysis and method used for this study is represented in fig. 1(a-i) which is the monthly variation of H components for all the geomagnetic stations.

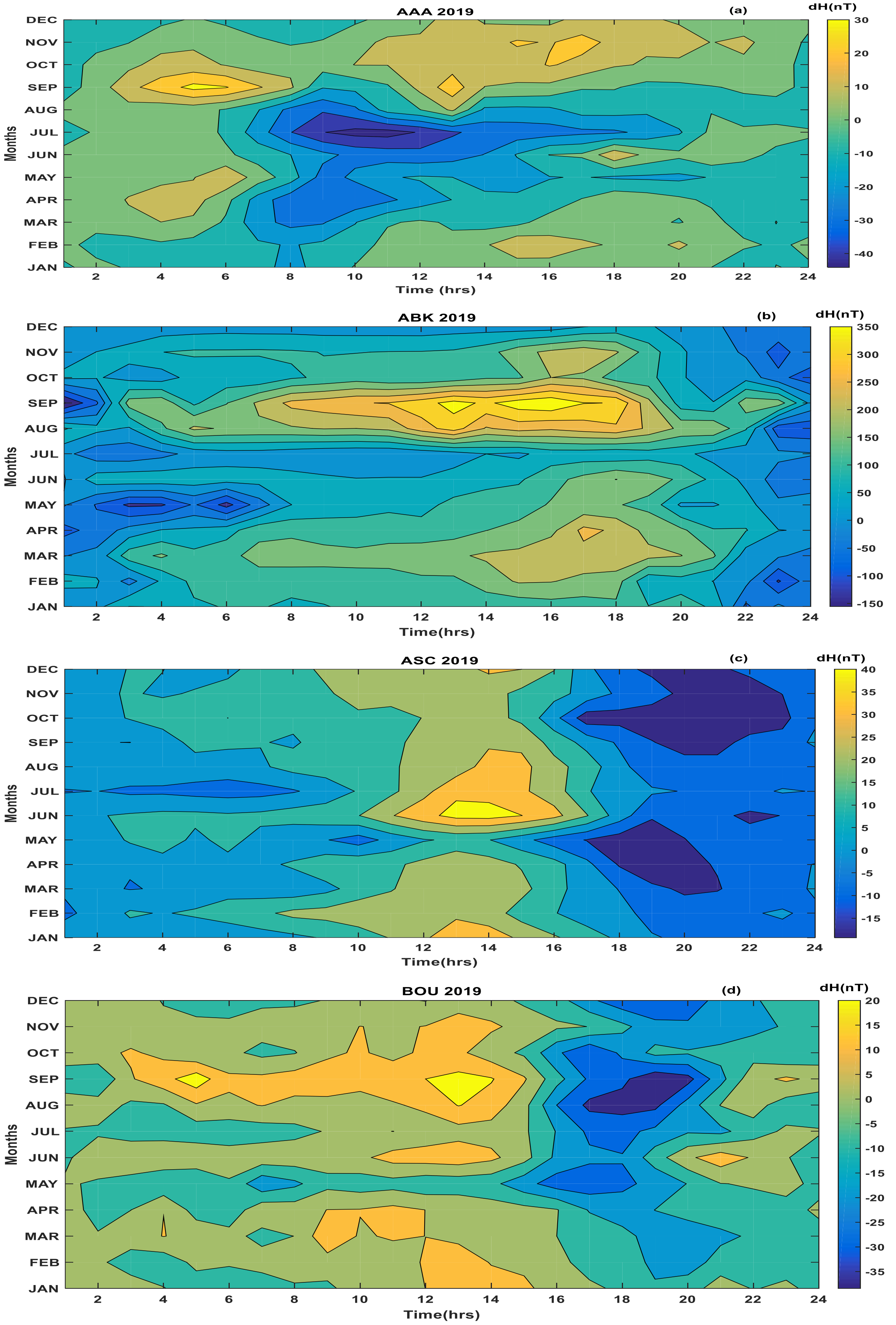

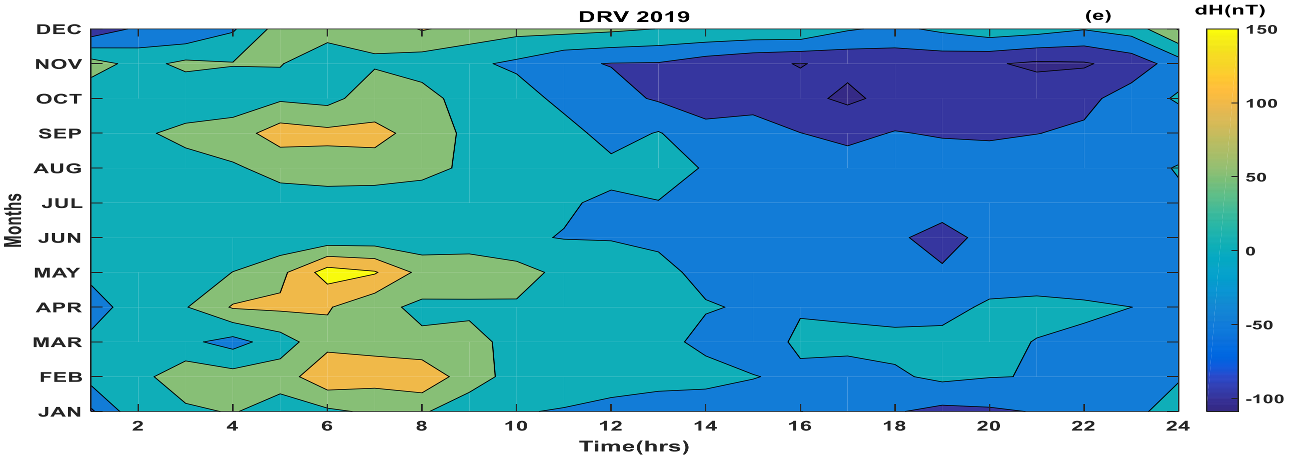
DRV 2019
(e)
dH(nT)
150
100
50
0
-50
-100
Months
DEC
NOV
OCT
SEP
AUG
JUL
JUN
MAY
APR
MAR
FEB
JAN
2
4
6
8
10
12
14
16
18
20
22
24
Time(hrs)

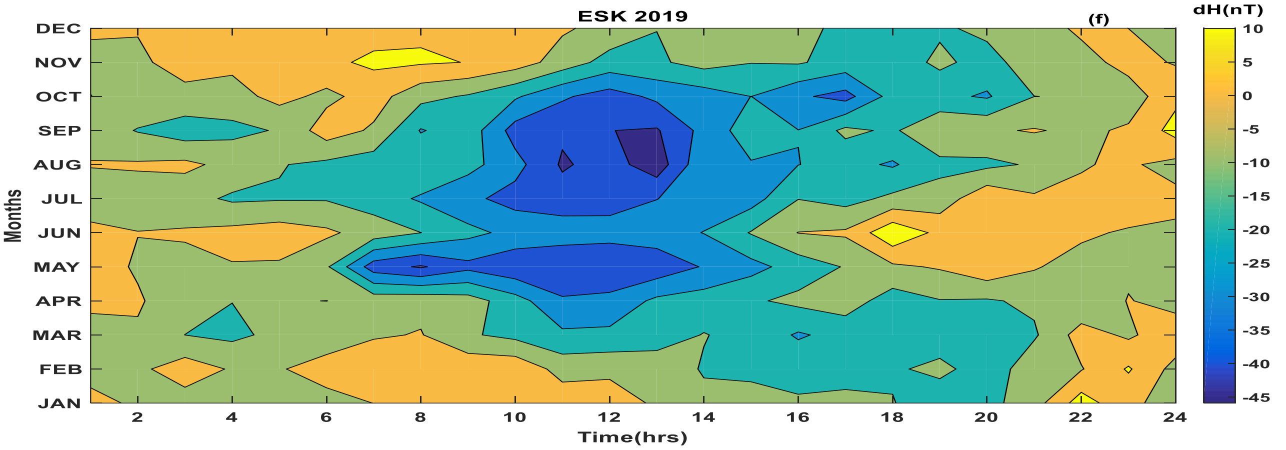
ESK 2019
(f)
dH(nT)
10
5
0
-5
-10
-15
-20
-25
-30
-35
-40
-45
Months
DEC
NOV
OCT
SEP
AUG
JUL
JUN
MAY
APR
MAR
FEB
JAN
2
4
6
8
10
12
14
16
18
20
22
24
Time(hrs)

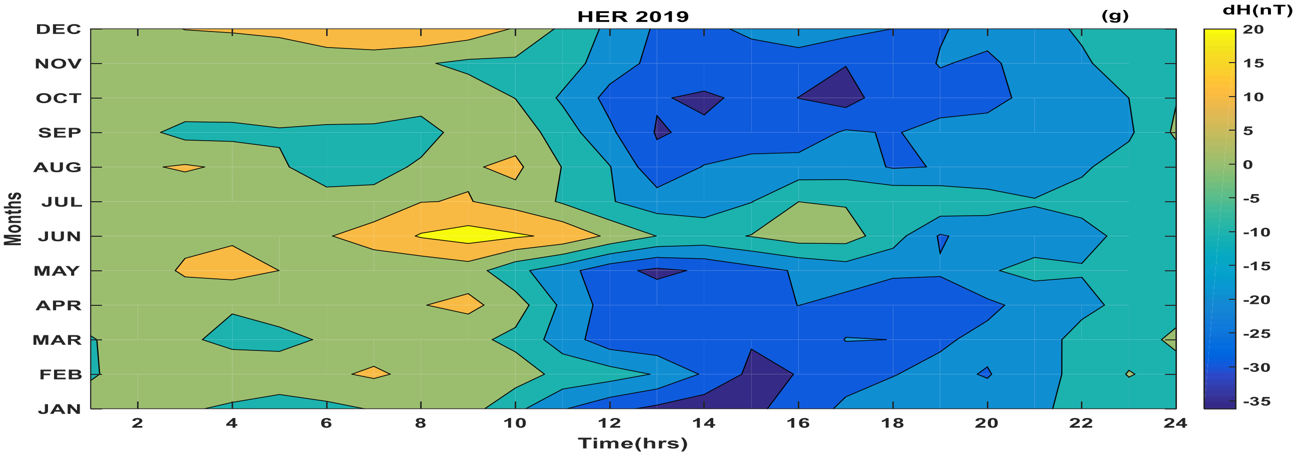
HER 2019
(g)
dH(nT)
20
15
10
5
0
-5
-10
-15
-20
-25
-30
-35
Months
DEC
NOV
OCT
SEP
AUG
JUL
JUN
MAY
APR
MAR
FEB
JAN
2
4
6
8
10
12
14
16
18
20
22
24
Time(hrs)

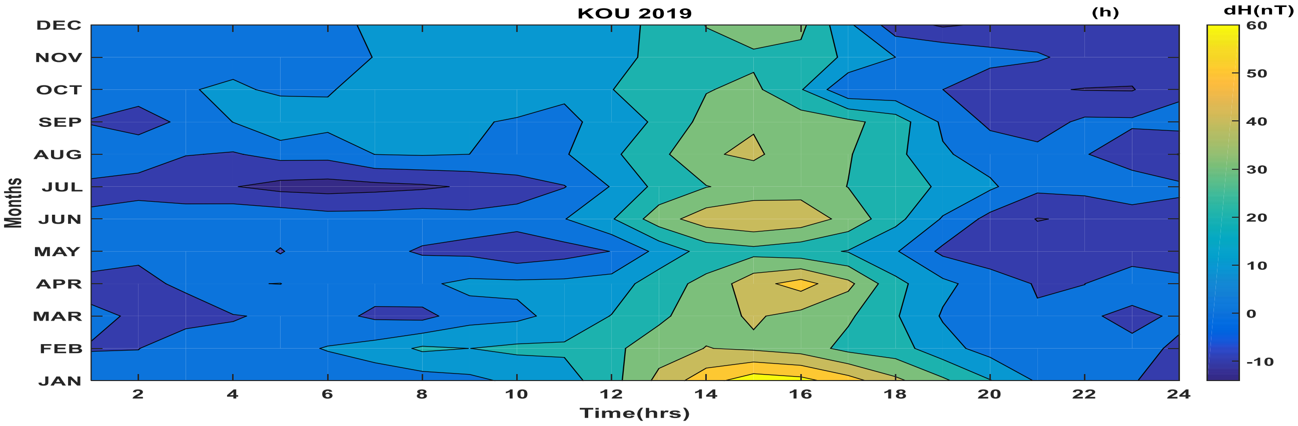
KOU 2019
(h)
dH(nT)
60
50
40
30
20
10
0
-10
Months
DEC
NOV
OCT
SEP
AUG
JUL
JUN
MAY
APR
MAR
FEB
JAN
2
4
6
8
10
12
14
16
18
20
22
24
Time(hrs)

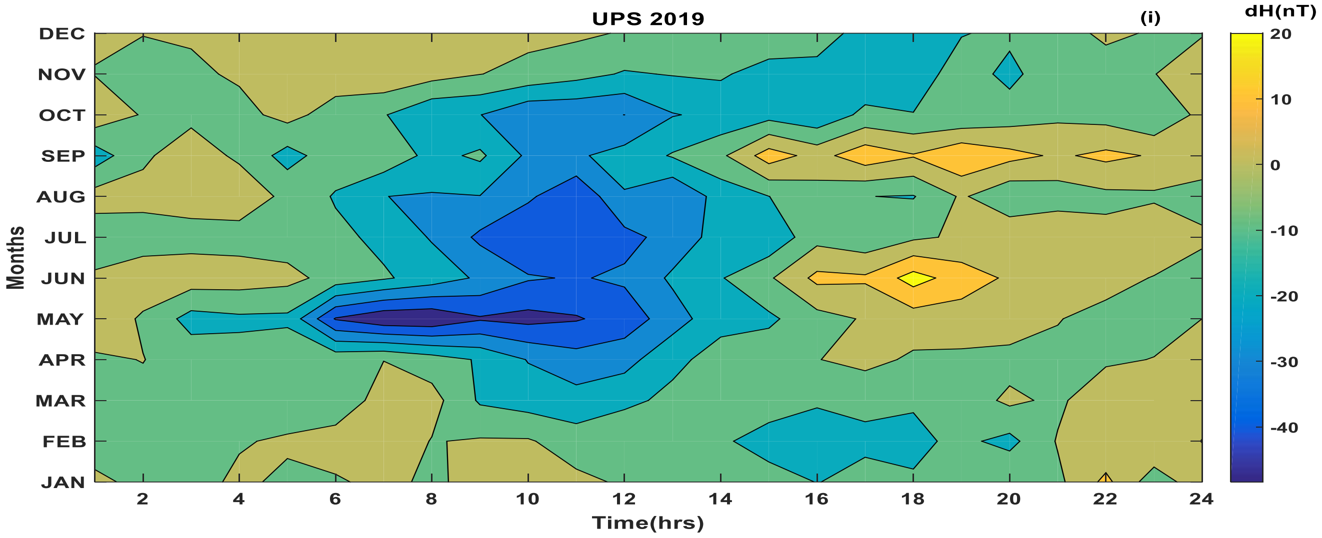

Fig. 1(a-i): The monthly variance of H component for all the geomagnetic stations

Fig. 1a (AAA) shows there is a low variation of geomagnetic disturbance notice across the year, both day and night (00hr-24:00hr)Lt. There is an enhancement of 30nT notice in September during the hour of 04:00-06:00Lt. as the maximum disturbance and the lowest disturbance of -40nT in July at the hour of 09:00-11:00Lt. This indicates that the region did not receive much geomagnetic disturbance as evidence that there is low solar activity marking the end of solar cycle 24 as recorded at the station.

At ABK, the situation was different, as geomagnetic disturbance was seen to be high during 08:00hr-18:00hr local time in September (see **fig.1b**). A maximum value of 350nT of H variation shows that solar activity at this latitude is still high as at the time of record in September. However, there is evidence of solar minimum across the year as recorded at this station.

The situation observed from ASC station shows there is minimal solar activity as the maximum geomagnetic disturbance was observed in June at 12:00hr-14:00hr local time (see **fig.1c**). There is a sign of solar minimum observed across the year as recorded at the station.

There is also a solar minimum situation across the year as recorded at BOU (**fig.1d**). A little enhancement was also observed in September during the hour of 12:00hr-14:00hr LT. The level of disturbance noticed at this station shows that solar activity is minimal.

Fig.1e (DRV) revealed low solar activity across the year with an enhancement noticed in February, May, and September during the hour of 06:00hr LT. A similar situation was also observed in ESK, HER, and UPS with low solar activity across the year. However, there is little enhancement notice in November by 08:00hr and June by 18:00hr LT at ESK (**see fig.1f**), 09:00hr in June at HER (**see fig.1g**) and 18:00hr in June at UPS (**see fig.1i**). Station KOU recorded a little bit of high disturbance at the hour of 14:00-16:00 LT across the year but with low solar activity.

Time Series Analysis

The time series analysis as shown in **Fig. 2(a-i)** indicates the nonlinear behavior of the system causing the effect observed in **Fig. 1(a-i)**. These fluctuations have been the reason for the temporal variation as witnessed across the world.

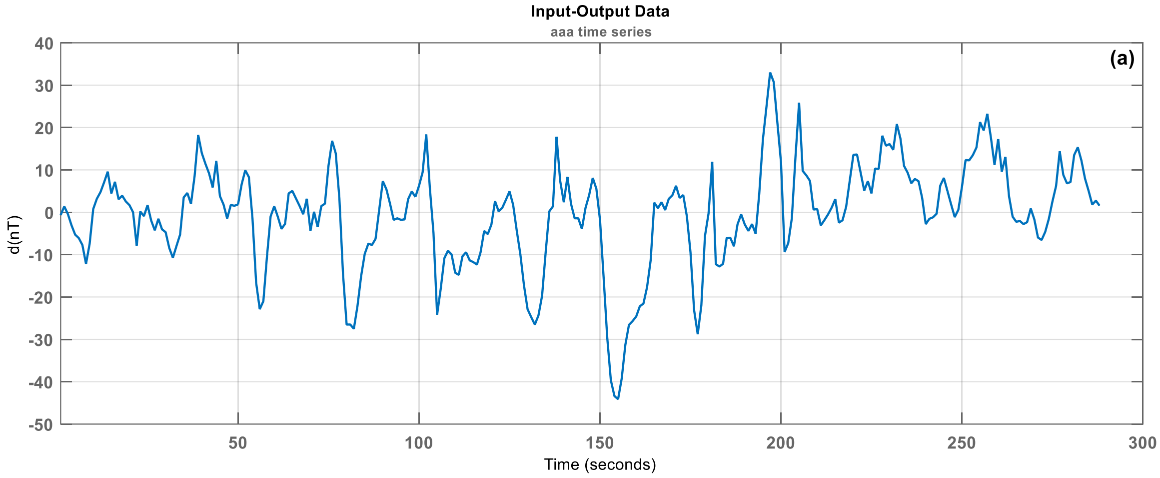
Input-Output Data
aaa time series
(a)
d(nT)
40
30
20
10
0
-10
-20
-30
-40
-50
50
100
150
200
250
300
Time (seconds)

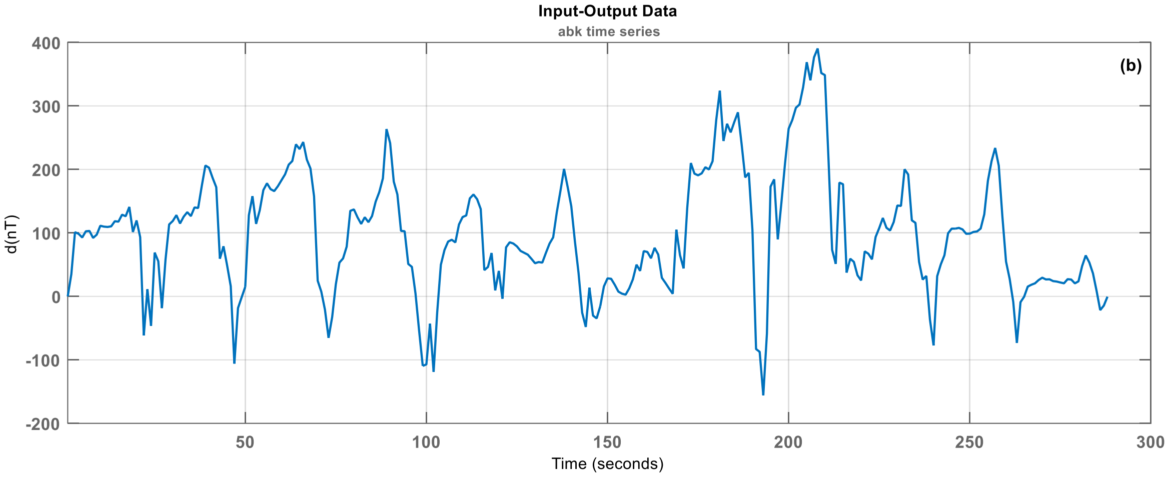
Input-Output Data
abk time series
(b)
d(nT)
400
300
200
100
0
-100
-200
50
100
150
200
250
300
Time (seconds)

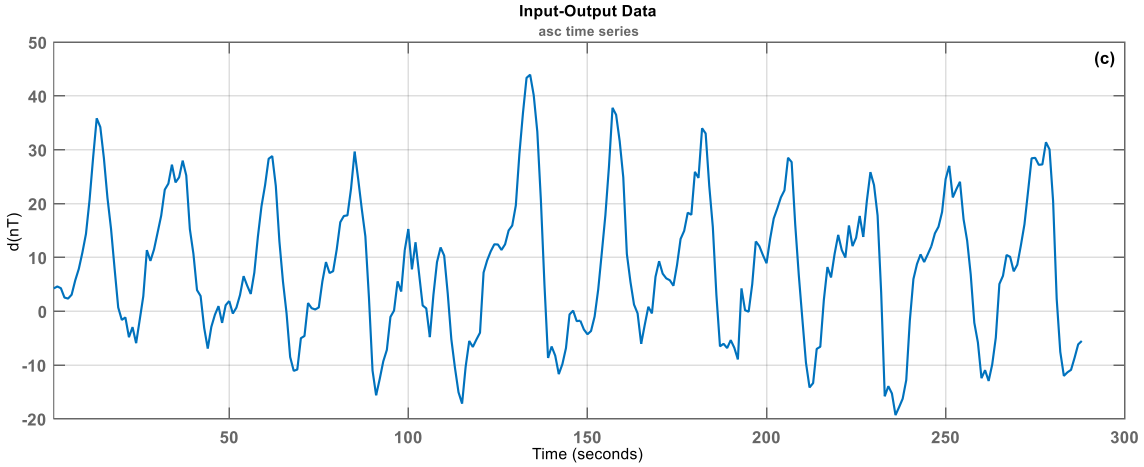
Input-Output Data
asc time series
(c)
d(nT)
50
40
30
20
10
0
-10
-20
50
100
150
200
250
300
Time (seconds)

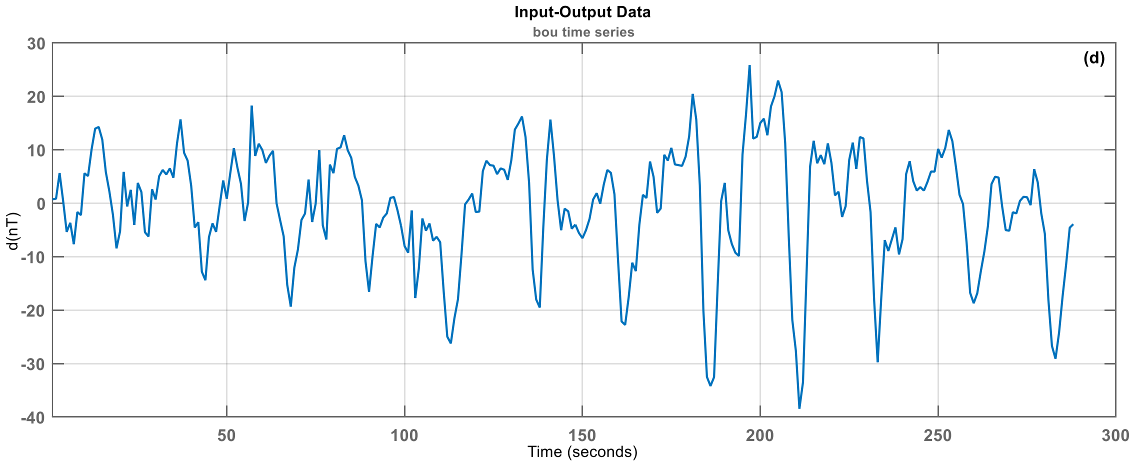
Input-Output Data
bou time series
(d)
d(nT)
30
20
10
0
-10
-20
-30
-40
50
100
150
200
250
300
Time (seconds)

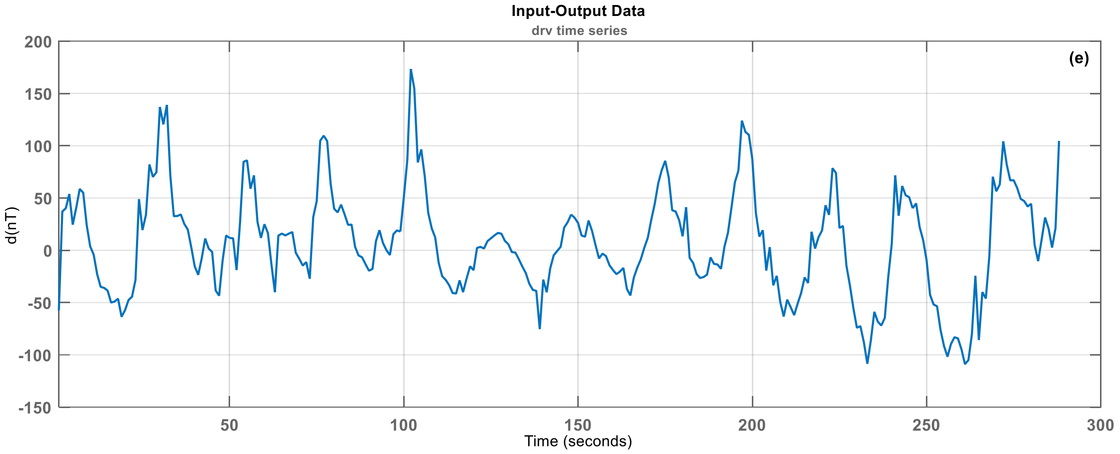
Input-Output Data
drv time series
(e)
d(nT)
200
150
100
50
0
-50
-100
-150
50
100
150
200
250
300
Time (seconds)

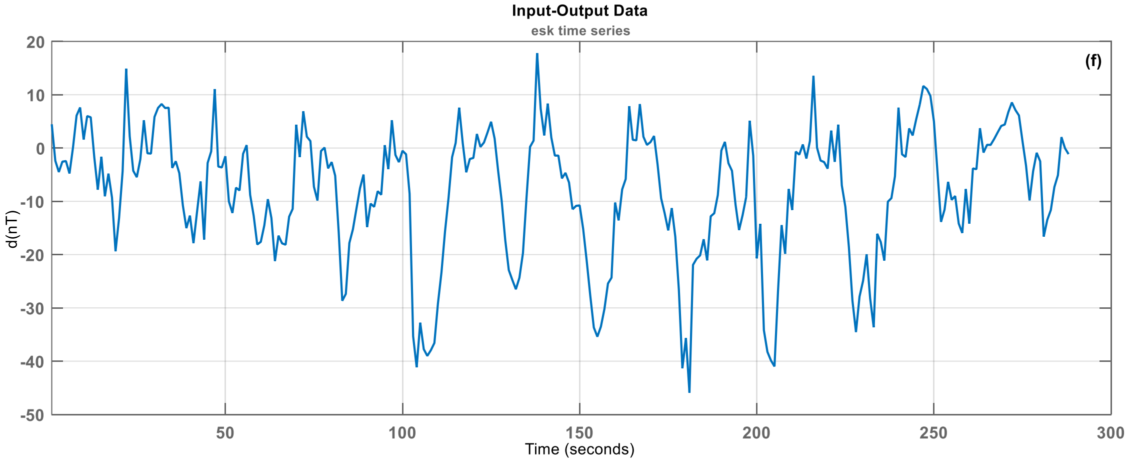
Input-Output Data
esk time series
(f)
d(nT)
20
10
0
-10
-20
-30
-40
-50
50
100
150
200
250
300
Time (seconds)

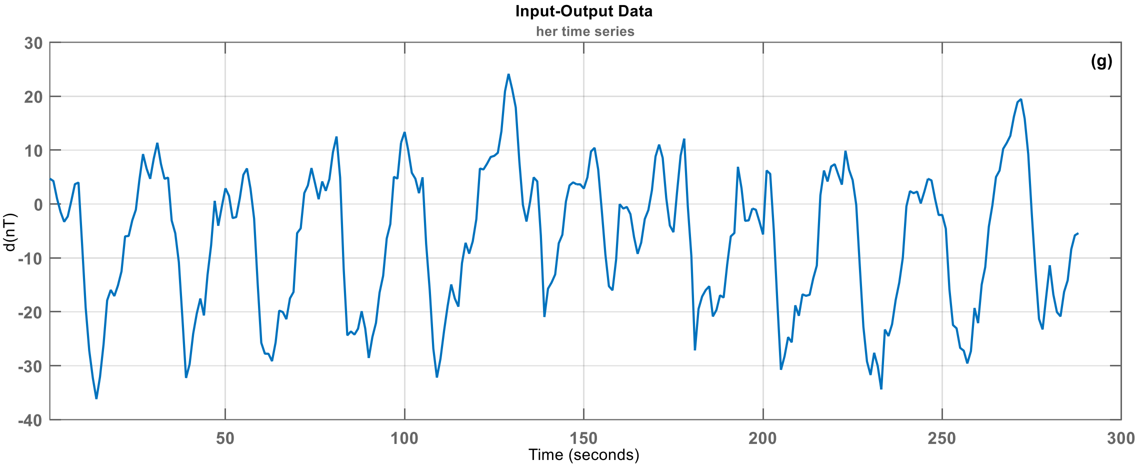
Input-Output Data
her time series
(g)
d(nT)
30
20
10
0
-10
-20
-30
-40
50
100
150
200
250
300
Time (seconds)

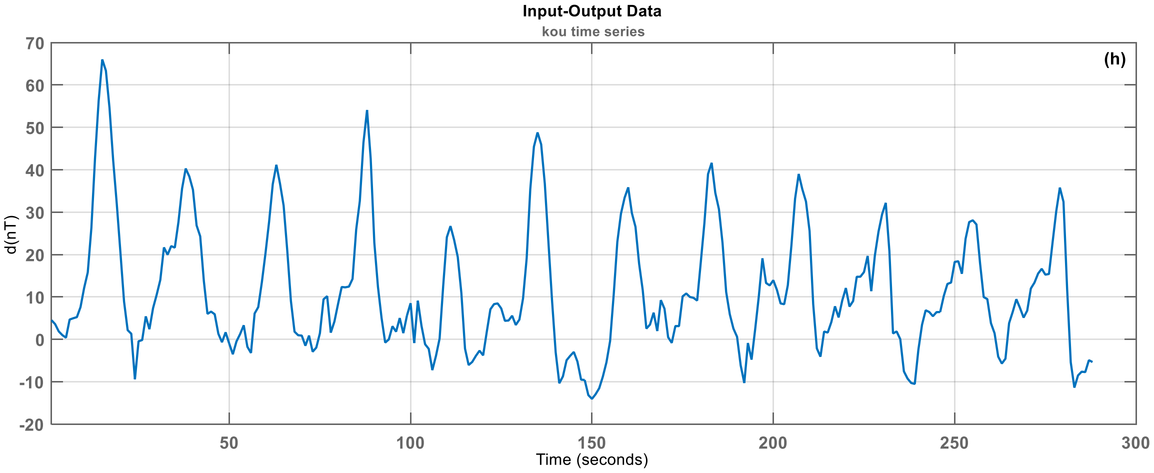
Input-Output Data
kou time series
(h)
d(nT)
70
60
50
40
30
20
10
0
-10
-20
50
100
150
200
250
300
Time (seconds)

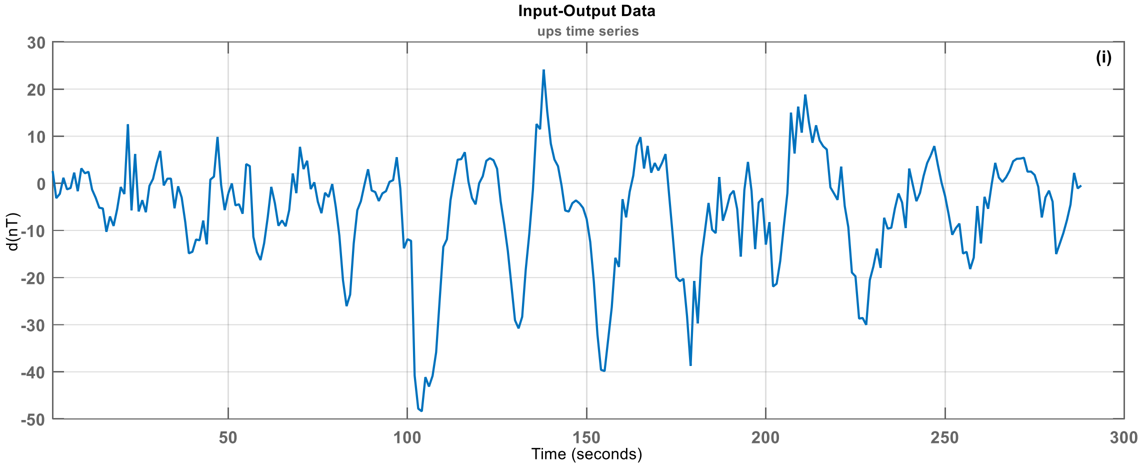

Fig. 2(a-i): The time series plot of dH for all the geomagnetic stations

The time series analysis of the temporal behavior of variable dH(t) is analyzed. The time series analysis behavior of variance in dH (t) across the stations shows higher fluctuations above 100nT for ABK and DRV as more disturbed while other stations have from 60nT below. This may be attributed to the temporal variation witnessed on the earth's geomagnetic field which can be called nonlinear system, observed on the magnetosphere due to the effect of solar activity. This indicates the temporal pattern of the system has been nonlinear and as it resulted from the ionosphere which is a region where natural processes occur. (Ogunsua et al., 2014; Pavlos et al. 1992).

CONCLUSION

This research study has been able to examine the solar activity at the minimum phase of solar cycle 24. Geomagnetic disturbed days data of 2019 obtained from nine stations across the globe have been analyzed using horizontal component H. From the result time series analysis, we affirmed that the temporal pattern of the system has been nonlinear due to the natural processes occurring in the ionosphere. Also from this study, it was revealed that solar activity during cycle 24 was minimal as it marks the end of the cycle. This was confirmed by the result obtained from analysis of data across all the stations which revealed low geomagnetic disturbance despite considering disturbed days. Apart from ABK which revealed high geomagnetic disturbance compared to other regions used for the study, the study agrees with past researches as to the end of solar cycle 24 with low solar activity. Therefore, this situation has accounted for the low geomagnetic disturbance on the earth's magnetosphere witnessed during the end period of solar cycle 24.

ACKNOWLEDGMENT

The authors acknowledge the International Real-Time Magnetic Observatory Network (INTERMAGNET) (http://www.intermagnet.org/) for making geomagnetic field data assessable for the stations used.

REFERENCE

1. Ajose, A.S and Falayi, E.O (2019). Analysis of Solar Quiet Horizontal Variation Using Wavelet Analysis During Year 2012. DUJOPAS 5(1a) pp. 85-94.
2. Campbell, W. (2003). Introduction to geomagnetic fields (2^{nd}). New York: Cambridge University Press.
3. Echer E, Gonzalez WD, Tsurutani BT (2011) Statistical studies of geomagnetic storms with peak Dst ≤ -50 nT from 1957 to 2008. J Atmos Sol TerrPhys 73(11–12):1454–1459. doi:1016/j.jastp.2011.04.21
4. Efimenko, V. M., & Lozitsky, V. G. (2023). Solar cycle 25 amplitude prediction based on sunspot

number increase rate. Advances in Space Research.

5. Falayi, E.O, Bolaji, O.S (2016), Variations of time derivatives of the horizontal geomagnetic field and horizontal geomagnetic field along the 96-degree magnetic meridian**,** Covenant Journal of Physical and Life Sciences (CJPL) Vol. 4 No 1 June, 2016
6. Falayi, E.O. Adepitan, J.O. and Oyebanjo O.A. (2017)**.** Geomagnetic field H, Z, and electromagnetic induction features of coronal mass ejections in association with geomagnetic storm at African longitudes. Canadian Journal of Physics, 96 (6): 654- 663, https://doi.org/10.1139/cjp-2017-0460.
7. Gopalswamy, N. (2022). The Sun and Space Weather. Atmosphere, 13(11), 1781.
8. Gray, L. J., Beer, J., Geller, M., Haigh, J. D., Lockwood, M., Matthes, K., White, W. (2010). Solar influences on climate. Reviews of Geophysics, 48(4).
9. Haigh, J.D, (2007), The Sun and the Earth’s Climate, Living Reviews in Solar Physics, 4 ISSN 2367-3648.
10. Hathaway, D. H. (2015). The solar cycle. Living reviews in solar physics, 12, 1-87.
11. Howard, T. (2014). Space weather and coronal mass ejections. Springer New York.
12. INTERMAGNET. (2019). International real-time magnetic observatory network. Available from http://www.intermagnet.org/.
13. Ishkov, V. N. (2018). Space weather and specific features of the development of current solar cycle. Geomagnetism and aeronomy, 58, 753-767.
14. Ishkov, V. N. (2021). Extreme space weather events during the first cycles of epochs with decreased solar activity. Geomagnetism and Aeronomy, 61, 801-809.
15. Miroshnichenko, L. (2023). Solar Activity. In Solar-Terrestrial Relations: From Solar Activity to Heliobiology (pp. 21-41). Cham: Springer International Publishing.
16. Moldwin M. (2008), An Introduction to Space Weather. Cambridge University Press, New York.
17. Moldwin, M. (2022). An introduction to space weather. Cambridge University Press.
18. Obiekezie, T. N, Obiadazie, S.C and Agbo, G.A (2013). Day-to-Day Variability of H and Z Components of the Geomagnetic Field at the African Longitudes. Hindawi publication dx.doi.org/10.1155/2013/909258.
19. Ogunsua, B. O., Laoye, J. A., Fuwape, I. A., and Rabiu, A. B.(2014): The comparative study of chaoticity and dynamical complexity of the low-latitude ionosphere, over Nigeria, during quiet and disturbed days, Nonlin. Processes Geophys., 21, 127–142,doi:10.5194/npg-21-127-2014, 2014.
20. Owens, M. J., Lockwood, M., Barnard, L. A., Scott, C. J., Haines, C., & Macneil, A. (2021). Extreme space-weather events and the solar cycle. Solar Physics, 296(5), 82.
21. Pavlos, G. P., Kyriakov, G. A., Rigas, A. G., Liatsis, P. I., Trochoutsos, P. C., and Tsonis A. A.(1992): Evidence for strange attractor structures in space plasmas, Geophysicae, 10, 309–322.
22. Petrovay, K. (2020). Solar cycle prediction. Living Reviews in Solar Physics, 17(1), 2.
23. Pulkkinen, A., Kataoka, R., Watari, S., Ichiki, M. (2010) Modeling geomagnetically induced current in Hokkaido, Japan. Advances in Space Research. 46: 1087-1093.
24. Rabiu, A.B., Mamukuyomi, A.I., Joshua, E.O., 2007. Variability of equatorial ionosphere inferred from geomagnetic field measurements. Bull. Astr. Soc. India 35, 607–618.
25. Reyes, P. I., Pinto, V. A., & Moya, P. S. (2021). Geomagnetic storm occurrence and their relation with solar cycle phases. Space Weather, 19(9), e2021SW002766.
26. Watari Shinichi (2019). Geomagnetic Storms of Cycle 24 and their Solar Sources. Earth, Planet, and Space 69:70 DOI. 10.1186/s40623-017-065z
27. Yamazaki, Y., Kosch, M.J., (2014) Geomagnetic lunar and solar daily variations during the last 100 years. J. Geophys. Res. Space Phys.119, 6732–6744.
28. Yamazaki, Y., Yumoto, K., Cardinal, M. G., Fraser, B. J., Hattori, P., Kakinami, Y., Liu, J. Y, Lynn, K. J. W., Marshall, R., McNamara, D., Nagatsuma, T., Nikiforov, V. M., Otadoy, R. E, Ruhimat, M., Shevtsov, B. M., Shiokawa, , Abe, S., Uozumi, T. & Yoshikawa, A. (2011). An empirical model of the quiet daily geomagnetic field variation. Journal of Geophysical Research, 116 (A10312), doi10.1029/2011JA016487.